ELSEVIER

Journal of Alloys and Compounds 465 (2008) 429–435

Journal of ALLOYS AND COMPOUNDS

www.elsevier.com/locate/jallcom

Effects of oxygen contents on the electrochromic properties of tungsten oxide films prepared by reactive magnetron sputtering

Horng-Hwa Lu *

Department of Mechanical Engineering, National Chin-Yi University of Technology, Taiping City, Taichung County 411, Taiwan, ROC

Received 4 September 2007; received in revised form 23 October 2007; accepted 23 October 2007
Available online 30 October 2007

Abstract

The electrochromism have been extensively investigated due to their potential applications such as smart window of architecture and automobile glazing to save energy and modulate the transmittance of light and solar radiation. The objective of this study is to investigate the effects of sputtering conditions on the microstructure and electrochromic properties of tungsten oxide films prepared by dc reactive magnetron sputtering. Experimental results showed that the deposition rate of WO_{3-y} films decreased with increasing oxygen flow rate. XRD and Raman spectra analysis suggests that the WO_{3-y} films deposited at various oxygen flow rates are poor crystallinity or amorphous. The transmission change between colored and bleached states at a wavelength of 550 nm was 61.4% as the oxygen content was 60%. The coloration efficiency slightly increases with increasing oxygen flow rate in the low oxygen content region and reaching a maximum value of 38.94 cm^2/C at 60% oxygen content. In addition, the films deposited at 60% oxygen content showed a good reversibility. The effects of lithium ions intercalated on the transmission of WO_{3-y} films were also discussed.
© 2007 Elsevier B.V. All rights reserved.

Keywords: Tungsten oxide; Sputtering; Electrochromic properties

1. Introduction

The effect and phenomenon that changes color of certain materials by an electrochemical reaction is called "electrochromism". The electrochromic devices modify its transmittance and reflectance in a reversible manner under the application of an external voltage [1]. Recently, many oxides of transition metals in the film form have been shown to possess electrochromic property and used in different fields including: (a) Non-illumination information display, (b) variable reflectance mirror, used for back mirror in automobile to anti-glazing, (c) smart window, and (d) variable emittance surface for aerospace industry [2].

Tungsten oxide is the most widely studied electrochromic material and devices. It has a nearly cubic structure which may be simply described as an "empty-perovskite" type formed by WO_3 octahedral that share corners. The empty space inside the cube is considerable and this provides the availability of a large number of interstitial sites where the guest ions can be inserted. Both amorphous and crystalline tungsten oxide thin films exhibit electrochromic coloration due to ionic insertion. In amorphous WO_3, the absorptance modulation during ion and electron insertion occurs in the visible and near-infrared regions of the spectrum. In crystalline WO_3, however, the injected electrons are to a significant extent delocalized and behave like free electrons, the free-electron like behavior results in a reflective optical modulation, which can be described by a modified Drude model [3].

It is generally accepted that the color change in the films to be related injection and extraction of electrons and metal cations, which can be written as [4]:

$$WO_{3-y} + xM^+ + xe^- = M_xWO_{3-y} \quad (1)$$

where M = H, Li, etc. The M_xWO_{3-y} films have intense blue, red, or golden color which depends on the x value and process of ion insertion and electron injection. Lee et al. [5] reported that a-WO_{3-y} films include mainly W^{6+} and W^{4+} states and the chemical formula can be written as ${W^{6+}}_{1-y}{W^{4+}}_yO_{3-y}$. The ion insertion reduced some W^{6+} states to W^{5+} states. The colored

* Tel.: +886 4 23924505x7179; fax: +886 4 23930681.
E-mail address: hhlu@ncut.edu.tw.

0925-8388/$ – see front matter © 2007 Elsevier B.V. All rights reserved.
doi:10.1016/j.jallcom.2007.10.105

films therefore contain W^{4+}, W^{5+}, and W^{6+} states and the optical absorption is caused by small polaron transitions between the W^{6+} and W^{4+} states and the W^{5+} states.

Various techniques are available for the preparation of tungsten oxide thin films for electrochromic application [6–12]. However, the effects of oxygen contents to the electrochromic properties of tungsten oxide films need more discussions. In the present paper, the reaction magnetron sputtering technique was used for the preparation of tungsten oxide thin films. The effects of oxygen content [flow ratio of $O_2/(Ar+O_2)$] to the microstructure and optical properties of WO_3 films were discussed. The relationships to the electrochromic properties were also reported.

2. Experimental procedures

2.1. Sample preparation

The tungsten oxide thin films were deposited from W metal target (99.95% purity, 7.62 cm in diameter, 0.64 cm in thickness, TELEDYNE, USA). The films were coated on ITO glass (80 Ω/□, RITEK) for properties analysis. Substrates were cut into dimensions of 20 mm × 20 mm, degreased and ultrasonically cleaned in acetone and alcohol, and subsequently dried in flowing nitrogen gas before deposition.

The reaction magnetron sputtering system is a rectangular vacuum chamber with tungsten metal targets. The target-to-substrate distance was 5 cm. The pressure was measured using a hot cathode ion gauge and a thermal couple vacuum gauge. Two separate mass flow controllers (MKS MFC-1179) were used to monitor the gas flow rate of argon and oxygen. A cryo-pump coupled with a rotary pump was used to achieve an ultimate pressure of 2.7×10^{-4} Pa before introducing gas mixtures of argon and oxygen. The targets were firstly pre-sputtered at 0.8 Pa for 10 min in Ar for cleaning. The deposition conditions were presented in Table 1.

2.2. Characterization

The thickness of deposited films was measured by surface profile meter (Alpha-Step200, TENCOR, USA) and then calculated the deposition rate. An X-ray photoelectron spectroscope (XPS, VG Scientific 210, West Sussex, UK) was used to investigate the composition of the films. The phase analysis of the films was determined by X-ray diffraction using Cu Kα radiation (XRD, Rigaku D/MAX2500, Tokyo, Japan). An atomic force microscope (AFM, DI Inc., USA) was used to observe the surface morphology and roughness. The bonding structures were measured by Raman spectrometer (LabRAM HR) with a 532.25 nm Ar laser. Optical properties were measured with an ultraviolet-visible-infrared spectrophotometer (Hitachi UV-2001) in the wavelength region of 300–1100 nm.

The electrochromic properties were characterized using cyclic voltammetry (CV) method. A standard three-electrode configuration consisting of the sample as the working electrode, a Pt counter electrode and a conventional saturated calomel electrode (SCE), was used to perform the electro-chemical tests. The electrolyte was a 0.1 M $LiClO_4$ propylene carbonate solution.

Table 1
Deposition conditions for WO_{3-y} films

Parameters	Values
Oxygen content [flow ratio of $O_2/(Ar+O_2)$]	33.3–66.7%
DC power of W target	100 Watt
Temperature of substrate	RT
Deposition pressure	0.4 Pa
Film thickness	300 nm

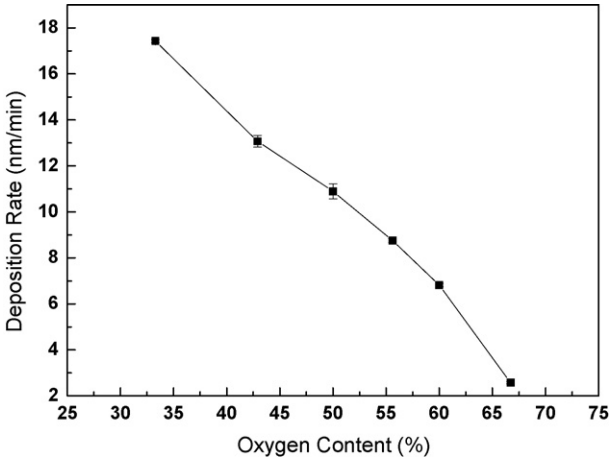

Fig. 1. Deposition rate of WO_{3-y} films vs. oxygen content. The total pressure and the dc power were 0.4 Pa and 100 W, respectively.

3. Results and discussions

3.1. Characteristics of WO_{3-y} films

The deposition rate of WO_{3-y} films vs. oxygen content is shown in Fig. 1. The results revealed that the deposition rate of WO_{3-y} films decreased with increasing oxygen flow rate. In general, higher $O_2/(Ar+O_2)$ flow ratio reduces the number of incident Ar ions on the W target. Besides, in the magnetron sputtering, higher content of oxygen increases the plasma impedance and decreasing the voltage difference between the cathode and the substrate. This can cause the smaller incident energy of Ar ions on the target. In addition, the formation of a ceramic compound on the metal target surface since the sputtering yield of oxide is much lower than pure metal, and cause a gradual decrease of deposition rate [13,14].

The quantitative XPS analysis of WO_{3-y} films with different oxygen contents are shown in Fig. 2. These results show that the variety of tungsten and oxygen composition is not obvious as oxygen content lower than 55%. The O:W ratios are about the value of 1.2. The O:W ratio increases to 1.67 when the oxy-

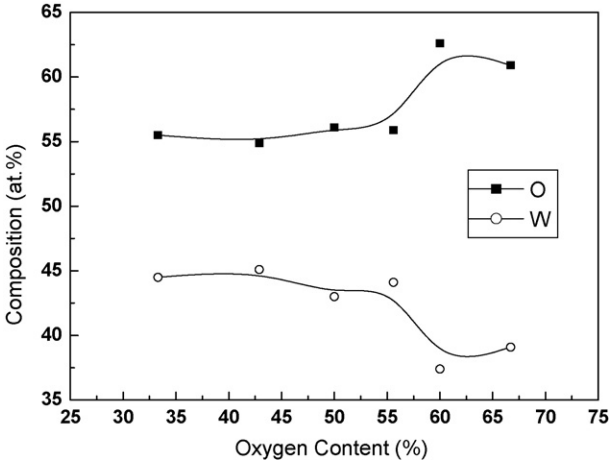

Fig. 2. The quantitative XPS analysis of WO_{3-y} films deposited at various oxygen contents.

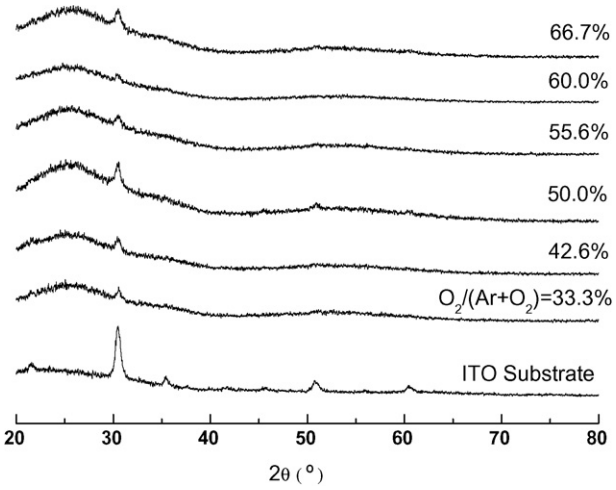

Fig. 3. X-ray diffraction patterns of WO_{3-y} films prepared at different oxygen contents.

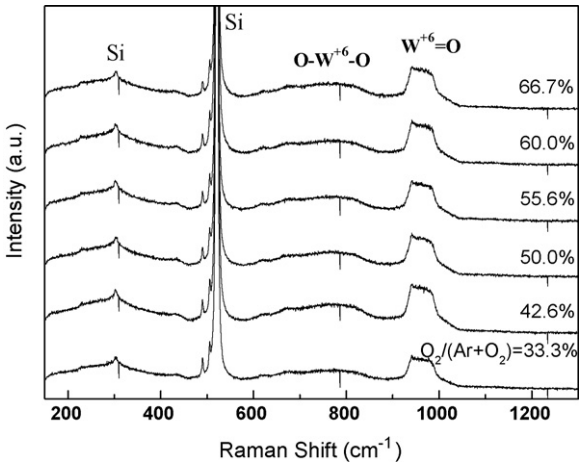

Fig. 4. Raman spectra of WO_{3-y} films prepared at various oxygen contents.

gen content is increased to 60%. It is well below stoichiometry when the films were prepared by reaction sputtering and using metallic mode target. Films prepared at low oxygen concentrations were metallic in appearance and gave no electrochromic response [15]. This means that the WO_{3-y} films with significant oxygen deficiency are not suitable for electrochromic devices.

X-ray diffraction patterns of WO_{3-y} films with different oxygen contents are shown in Fig. 3. The pattern consists of a broad hump with no well-defined diffraction peaks, except the

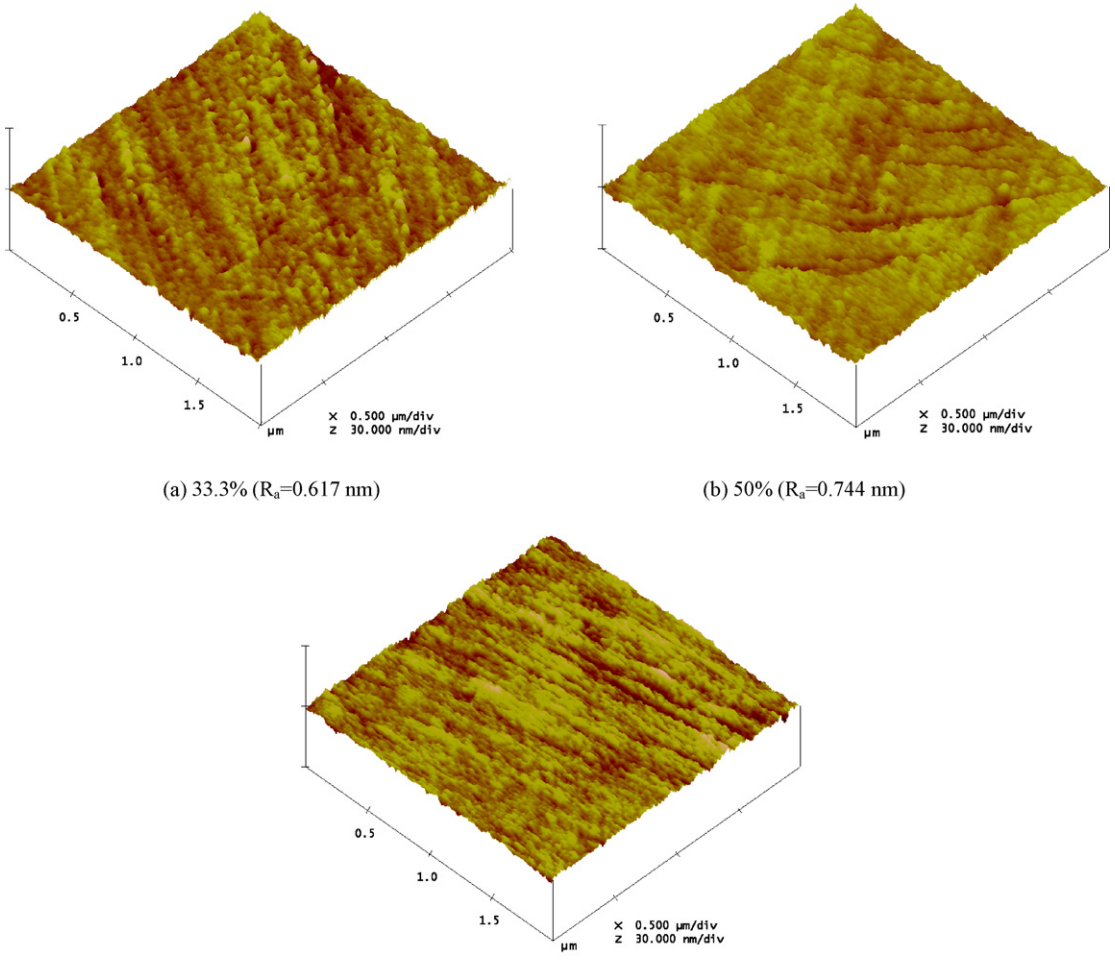

(a) 33.3% (R_a=0.617 nm)

(b) 50% (R_a=0.744 nm)

(c) 60% (R_a=0.666 nm)

Fig. 5. AFM images showing the morphology and roughness of WO_{3-y} films prepared at various oxygen contents.

superposed diffraction peaks of the ITO substrate, indicating that the film is of poor crystallinity. The amorphous-envelope diffraction pattern may result from the amorphous property and internal stress of a-WO_3 films, which is usually a property of films prepared by sputter-deposition at room temperature [16].

Fig. 4 is the Raman spectra of WO_{3-y} films prepared at various oxygen contents. The spectrums of all samples show an obvious peak at 950 cm^{-1}, which has been assigned to the W^{6+}=O stretching mode of terminal oxygen atoms possible on the surfaces of the cluster and micro-void structure in the film [17]. Salje had reported that the Raman spectrum of crystalline WO_3 had two strongest peaks, 719 and 807 cm^{-1} [18]. The O–W^{6+}–O bonds at 770 cm^{-1}, which traces the origin back of the crystalline WO_3 peaks, was also reported by Shigesato et al. [19]. There is a relatively broad hump between 600 and 900 cm^{-1} in Fig. 4. It suggests that the WO_{3-y} films deposited at various oxygen flow rates are poor crystallinity or amorphous. These results are consistent with the XRD analysis in Fig. 3.

Fig. 5 shows AFM images of WO_{3-y} films deposited at different oxygen contents. Results indicated that the surface morphology is flat and dense. The values of R_a are lower than 1 nm for all samples. These results show that the variety of roughness is not obvious with increasing oxygen contents.

3.2. Electrochromic properties

Fig. 6 shows the transmission spectra of WO_{3-y} films deposited at various oxygen contents in the as-deposited, colored, and bleached state. The WO_{3-y} films that deposited at deferent oxygen contents are transparent. The color of the films changes to dark blue when Li^+ ions and electrons are electrochemically injected into these films. This is because of the larger charge capacity of a-WO_3, which could be due to thermally induced defects possibly related to oxygen substoichiometry [20]. The specimens show good coloration behavior in the visible and NIR region. The oscillations behavior of transmission spectra is interference effect due to the thickness of WO_{3-y} films [21]. The electrochromic materials change their optical properties due to the action of an electric field, and can be changed back to the original state by a reverse electric field. The reversible reaction can be described as [4]:

$$WO_3(\text{transparent}) + x(M^+ + e^-) \leftarrow (\text{voltage}) \rightarrow M_xWO_3(\text{blue}). \quad (2)$$

The specimen deposited at 60% oxygen content shows a good reverse phenomenon between the coloration and bleached state indicating that the specimen has good electrochromic properties.

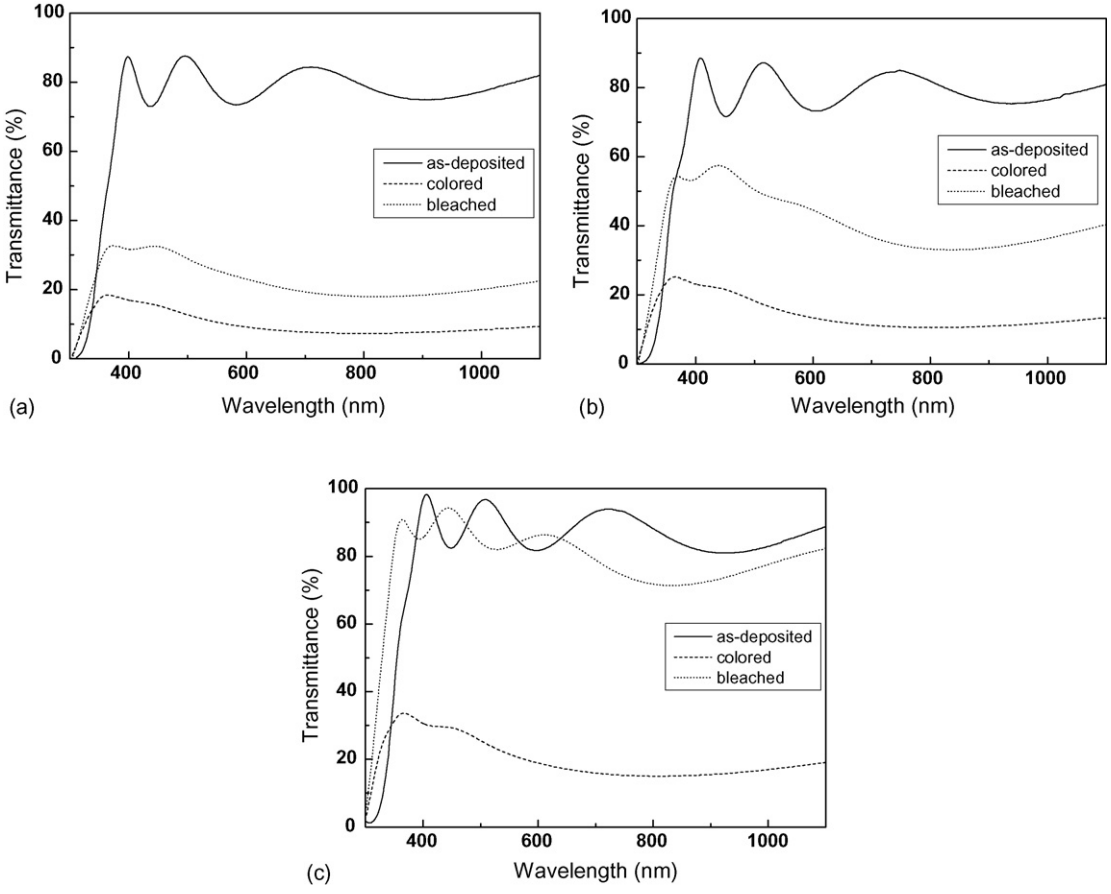

Fig. 6. Transmittance spectra of WO_{3-y} films deposited at various oxygen flow rates of (a) 33.3%, (b) 50%, (c) 60% in the as-deposited, colored and bleached state.

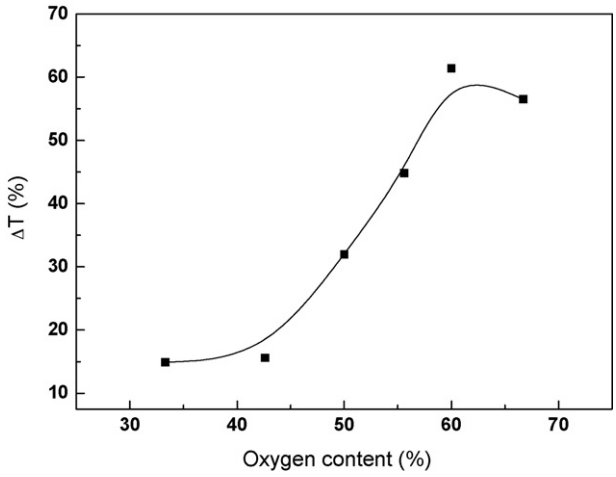

Fig. 7. The transmission modulation at 550 nm of the WO_{3-y} films deposited at various oxygen contents.

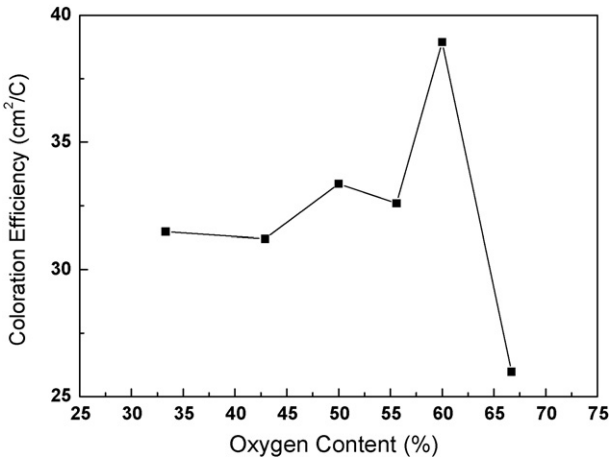

Fig. 9. The coloration efficiency of WO_{3-y} films prepared at different oxygen contents.

However, the specimen deposited at 33.3% oxygen content did not be bleached effectively.

The difference of transmittance between colored and bleached at 550 nm of the WO_{3-y} films deposited at various oxygen contents is shown in Fig. 7. Results indicated that the difference of transmittance increased with the increase the oxygen content. The transmission change of maximum between colored and bleached states at a wavelength of 550 nm was 61.4% as the oxygen content was 60%. Hutchins et al. [15] had reported that the films deposited at lower oxygen concentrations were not suitable for electrochromic devices due to the significant oxygen deficiency. Similar results were previously reported by Brigouleix et al. [22].

Fig. 8 is the optical density change (ΔOD) of WO_{3-y} films prepared at various oxygen contents. The optical density means the light absorption ability of electrochromic films and ΔOD is the solar optical density change.

$$\Delta\mathrm{OD} = \frac{\log T_{\mathrm{bleaching}}}{\log T_{\mathrm{coloring}}} \tag{3}$$

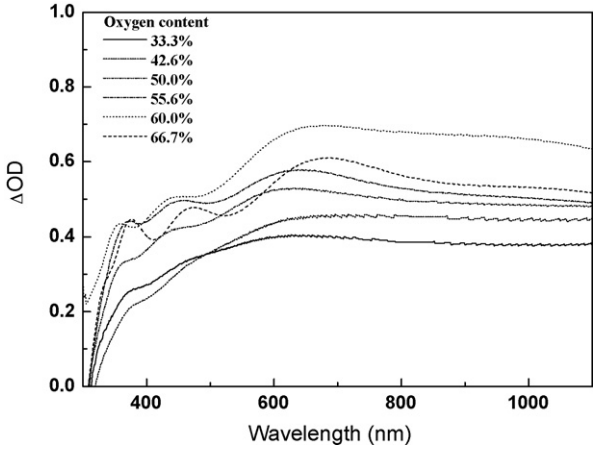

Fig. 8. Optical density change of WO_{3-y} films deposited at different oxygen contents.

where $T_{\mathrm{bleaching}}$ and T_{coloring} are transmittance of bleached state and colored state, respectively.

Coloration efficiency of electrochromic films is an important index for their application and fabrication. The coloration efficiency could be given by

$$\mathrm{CE} = \frac{\Delta\mathrm{OD}}{Q_{\mathrm{in}}} \tag{4}$$

where Q_{in} is the injected charge per unit area. The coloration efficiency thus obtained at 550 nm is plotted as a function of oxygen content in Fig. 9. It shows that the coloration efficiency slightly increases with increasing oxygen content in the low oxygen content region and reaching a maximum value of 38.94 $\mathrm{cm^2/C}$ at 60%. High coloration efficiency of electrochromic film means that the devices have better optical regulation by less injected charge and causing a better stability and reproducibility of colored/bleached cycles.

The first three cyclic voltammograms of WO_{3-y} films deposited at various oxygen contents are shown in Fig. 10. The scan rate of measurements was 20 mV/s in the −1.5 and 1 V range. It is known that [23], the electrochromic films were colored by charge injection and a part of this charge was extracted during the subsequent bleaching process. By repeating the colored/bleached cycles, a saturated state is achieved whereas the amount of injected charge is equal to extracted charge. In this experiment, the WO_{3-y} films that were deposited at 60% oxygen contents show a good electrochemical stability as Li^+ ion can be almost inserted and extracted reversibly in the cycling test.

The number of Li^+ ions per W atom, x, was calculated from the expression given by

$$x = \frac{Q_{\mathrm{Li}}}{Ad}\frac{M}{eN_{\mathrm{a}}\rho} \tag{5}$$

Q_{Li} is the total charge of the intercalated lithium ions. Here A is the area, d the thickness, M the molar mass and ρ is the density of the oxide films. The constant e and N_{a} are the elementary charge and the Avogadro constant, respectively. The

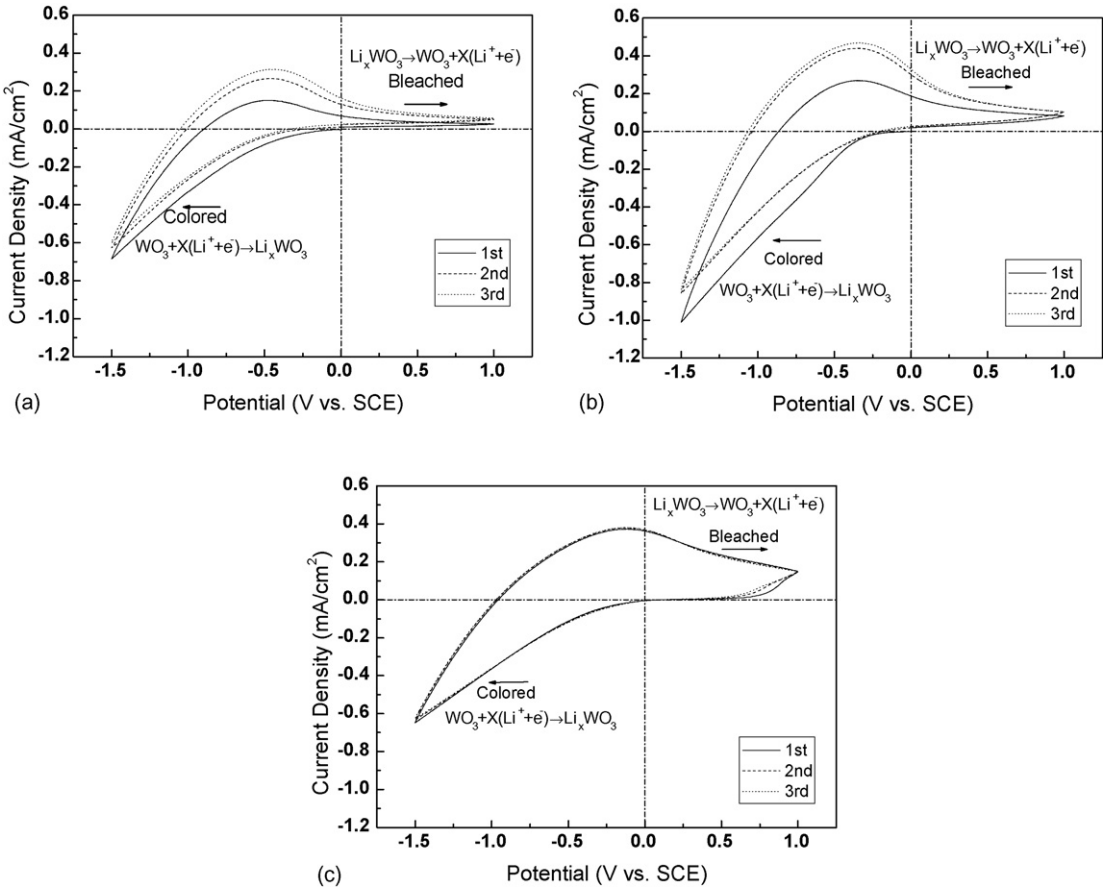

Fig. 10. Cyclic voltammograms of WO_{3-y} films deposited at various oxygen contents of (a) 33.3%, (b) 50% and (c) 60%.

effects of lithium ions intercalculated on the transmission of WO_{3-y} films that deposited at 60% of oxygen content are shown in Fig. 11. It is seen that transmittance decreases with increasing Li^+ intercalation. This decrease is due to the absorption by W^{5+} in amorphous tungsten oxide films [24]. The insertion of Li^+ in WO_{3-y} films breaks up the continuous random W–O–W network to form Li_xWO_{3-y} compound, as described in Eq. (1) and called tungsten bronze. This behavior has been attributed to the number of W^{6+} sites of final states available for the electron involved in the transition obviously decreases as more Li is intercalated.

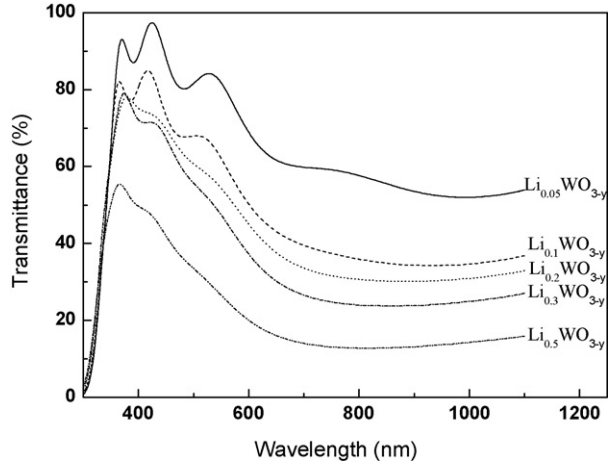

Fig. 11. Transmittance as a function of wavelength for lithium intercalated WO_{3-y} film deposited in argon with 60% oxygen content, 100 W and 0.4 Pa.

4. Conclusions

The deposition rate of WO_{3-y} films decreased with increasing oxygen content. From X-ray analysis and Raman spectra results show that the WO_{3-y} films deposited at various oxygen contents are poor crystallinity or amorphous and the dominant bonding are W^{6+}=O type. The variation of surface roughness is not obvious with increasing oxygen contents. The color of the films changes to dark blue when Li^+ ions and electrons are electrochemically injected into these films. The specimens show good coloration behavior in the visible and NIR region. The specimen deposited at 60% oxygen content shows a good reverse phenomenon between the coloration and bleached state. The WO_{3-y} films that deposited at 60% oxygen contents shows a good electrochemical stability as Li^+ ion can be almost inserted and extracted reversibly in the cycling test.

Acknowledgement

The authors would like to thank the National Science Council of the Taiwan, Republic of China, for its financial support under Contract No. NSC 95-2221-E-167-007.

References

[1] P.R. Somani, S. Radhakrishnan, Mater. Chem. Phys. 77 (2002) 117.
[2] C.G. Granqvist, E. Avendano, A. Azens, Thin Solid Films 442 (2003) 201.
[3] J.S.E.M. Svensson, C.G. Granqvist, Thin Solid Films 126 (1985) 31.
[4] B.W. Faughnan, R.S. Crandall, P.M. Heyman, RCA Rev. 36 (1975) 177.
[5] S.H. Lee, H.M. Cheong, J.G. Zhang, A. Mascarenhas, D.K. Benson, S.K. Deb, Appl. Phys. Lett. 74 (2) (1999) 242.
[6] C.W. Ong, H.Y. Wong, G.K.H. Pang, K.Z. Baba-Kishi, C.L. Choy, J. Mater. Res. 16 (6) (2001) 1541.
[7] J.L. He, M.C. Chiu, Surf. Coat. Technol. 127 (2000) 43.
[8] L. Meda, R.C. Breitkopf, T.E. Haas, R.U. Kirss, Thin Solid Films 402 (2002) 126.
[9] G. Leftheriotis, S. Papaefthimiou, P. Yianoulis, Solar Energy Mater. Solar Cells 83 (2004) 115.
[10] M. Deepa, A.K. Srivastava, S. Singh, S.A. Agnihotry, J. Mater. Res. 19 (9) (2004) 2576.
[11] A. Rougier, F. Portemer, A. Quédée, M. El Marssi, Appl. Surf. Sci. 153 (1999) 1.
[12] M. Regragui, M. Addou, A. Outzourhit, J.C. Bernéde, Elb. El Idrissi, E. Benseddik, A. Kachouane, Thin Solid Films 358 (2000) 40.
[13] S.K. Habib, A. Rizk, I.A. Mousa, Vacuum 49 (1998) 153.
[14] S.M. Rossnagel, J.J. Cuomo, W.D. Westwood, Handbook of Plasmas Processing Technology, Park Ridge, NJ, USA, 1982.
[15] M.G. Hutchins, N.A. Kamel, K. Abdel-Hady, Vacuum 51 (1998) 433.
[16] X.G. Wang, Y.S. Jiang, N.H. Yang, L. Yuan, S.J. Pang, Appl. Surf. Sci. 143 (1999) 135.
[17] J.V. Gabrusenoks, P.D. Chikmach, A.R. Lusis, J.J. Kleperis, G.M. Ramans, Solid State Ionics 14 (1984) 25.
[18] E. Salje, Acta Crystallogr. A 31 (1975) 360.
[19] Y. Shigesato, A. Murayama, T. Kamimori, K. Matsuhiro, Appl. Surf. Sci. 33/34 (1988) 804.
[20] F. Cogan, T.D. Plante, M.A. Parker, R.D. Raugh, J. Appl. Phys. 60 (8) (1986) 2735.
[21] D. Yang, L. Xue, Thin Solid Films 469/470 (2004) 54.
[22] C. Brigouleix, P. Topart, E. Bruneton, F. Sabary, G. Nouhaut, G. Campet, Electrochim. Acta 46 (2001) 1931.
[23] M. Kitao, S. Yamada, S. Yoshida, H. Akram, K. Urabe, Solar Energy Mater. Solar Cells 25 (1992) 241.
[24] G.A. Niklasson, L. Berggren, A.L. Larsson, Solar Energy Mater. Solar Cells 84 (2004) 315.